

See discussions, stats, and author profiles for this publication at: <https://www.researchgate.net/publication/41464677>

# Quantum Tunneling of Hydrogen Atom in Dissociation of Photoexcited Methylamine

ARTICLE in THE JOURNAL OF PHYSICAL CHEMISTRY A · FEBRUARY 2010

Impact Factor: 2.69 · DOI: 10.1021/jp912107h · Source: PubMed

CITATIONS

17

READS

44

## 7 AUTHORS, INCLUDING:



**S. Rosenwaks**

Ben-Gurion University of the Negev

257 PUBLICATIONS 3,485 CITATIONS

SEE PROFILE



**Yehuda Zeiri**

Ben-Gurion University of the Negev

132 PUBLICATIONS 2,176 CITATIONS

SEE PROFILE



**Ronnie Kosloff**

Hebrew University of Jerusalem

440 PUBLICATIONS 15,526 CITATIONS

SEE PROFILE



**Ilana Bar**

Ben-Gurion University of the Negev

172 PUBLICATIONS 2,264 CITATIONS

SEE PROFILE

Quantum Tunneling of Hydrogen Atom in Dissociation of Photoexcited Methylamine<sup>†</sup>Ran Marom,<sup>‡</sup> Chen Levi,<sup>‡</sup> Tal Weiss,<sup>‡</sup> Salman Rosenwaks,<sup>‡</sup> Yehuda Zeiri,<sup>§</sup> Ronnie Kosloff,<sup>||</sup> and Ilana Bar<sup>\*,\*</sup>

Department of Physics, Ben-Gurion University, Beer Sheva 84105, Israel, Department of Biomedical Engineering, Ben-Gurion University, Beer Sheva 84105, Israel and Department of Chemistry, NRCN, Beer-Sheva 84190, Israel, Department of Physical Chemistry and the Fritz Haber Center for Molecular Dynamics, The Hebrew University of Jerusalem, Jerusalem 91904, Israel

Received: December 23, 2009; Revised Manuscript Received: January 29, 2010

The probability of hydrogen atom release, following photoexcitation of methylamine, CH<sub>3</sub>NH<sub>2</sub>, is found to increase extensively as higher vibrational states on the first excited electronic state are accessed. This behavior is consistent with theoretical calculations, based on the probability of H atom tunneling through an energy barrier on the excited potential energy surface, implying that N–H bond breaking is dominated by quantum tunneling.

## I. Introduction

Photodissociation of polyatomic molecules is of fundamental interest and widely studied.<sup>1–9</sup> Often, different parameters affect and characterize the photodissociation of a particular molecule; these may include: availability of different dissociation channels, time scales of fragment separation, initial and final states of excitation, the intensity, polarization and energy of the used photons, and the involved potential energy surfaces (PESs) and the coupling between them as well as the presence of energy barriers along the different reaction paths. The existence of energy barriers has a major effect on the release of light atoms during photodissociation. However, their role and influence on the detailed dynamical picture is still not completely understood.

One appealing system for photodissociation studies is the methylamine (CH<sub>3</sub>NH<sub>2</sub>) molecule, which figures extensively in organic and biologic building blocks, and accordingly might have implications on our understanding of photoinduced processes in molecules containing amino moieties. Already in the 1960s,<sup>10</sup> it was proposed that the photodissociation of methylamine, following broad-band excitation in the 194–244 nm range, leads to a dominant (at least 75%) N–H bond fission, together with smaller contributions from both the C–N (<5%) and C–H (~7.5%) bond fission channels and the H<sub>2</sub> (<10%) elimination pathway. In a more recent photofragment translational spectroscopy (PTS) study of the 222 nm photolysis of CH<sub>3</sub>NH<sub>2</sub>, evidence for the same primary channels was found, whereas all four were found to be significant.<sup>11</sup> Furthermore, H(D) Rydberg atom photofragment translational spectroscopy studies indicated that most, if not all, of the observed H(D) atoms arise as a result of N–H (N–D) bond fission,<sup>12</sup> consistent with the earlier estimates of the relative importance of the different fragmentation channels.<sup>10</sup> Similar results were also found by measuring the relative H/D atom yields resulting in our vibrationally mediated photodissociation studies.<sup>13</sup> For example, we found that the ~243.1 nm dissociation of CD<sub>3</sub>NH<sub>2</sub> pre-excited with one N–H stretch quanta, corresponding to a

combined (vibration + UV) excitation energy of ~44 520 cm<sup>-1</sup>, leads to a H/D ratio of about 15. This ratio was found to decrease as higher initial vibrational states were pre-excited. Moreover, we have found that the H/D ratio, obtained following promotion of vibrationless ground state CD<sub>3</sub>NH<sub>2</sub> molecules to analogous vibronic states (excitation energies of 41 625–45 000 cm<sup>-1</sup>) decreases gradually from about 28 to 14, as higher states are accessed.<sup>14</sup> Also, theoretical calculations suggested that the transition states on the excited PES are the lowest during N–H rupture, implying its dominant dissociation.<sup>15</sup> The fragments resulting from N–H bond fission were considered to arise following H atom tunneling through an early barrier on the first excited electronic state,  $\tilde{A}$ , and a conical intersection (CI) between the  $\tilde{A}$  and ground electronic,  $\tilde{X}$ , states.<sup>12,15,16</sup> The occurrence of N–H bond dissociation via tunneling was also manifested by the large influence of the NH/ND substitution, in methylamine isotopologues, on the predissociation lifetime.<sup>17–19</sup> Particularly, it was found that the lifetime of the excited deuterated isotopologue, CH<sub>3</sub>ND<sub>2</sub> (8.8 ps), at its origin is about 20 times longer than that of CH<sub>3</sub>NH<sub>2</sub> (0.38 ps).<sup>17,18</sup>

In this work we report the first study on the dissociation probability of methylamine to release hydrogen photofragments. We take a new approach, which provides a quantitative treatment of tunneling, by comparing the experimental results with those of an analytical model and with direct dynamic calculations. The dissociation probabilities were examined for excitations to different final vibrational states on the first bound electronic state. It was found that the dissociation probability increases as higher vibrational states on the upper electronic state are accessed. This supports the suggestion and is consistent with our theoretical predictions, based on the probability of the H atom tunneling on the excited PES, that hydrogen release is dominated by a tunneling process.

## II. Methods

**a. Experimental Section.** The experimental apparatus consists of a home-built time-of-flight mass spectrometer (TOFMS) and two different ultraviolet (UV) tunable laser beams for excitation of the methylamine molecules to the  $\tilde{A}$  state and for ionization of the H photofragments, respectively. The excitation schemes employed in the experiment are described below and

<sup>†</sup> Part of the “Reinhard Schinke Festschrift”.

<sup>\*</sup> Corresponding author. E-mail: ibar@bgu.ac.il.

<sup>‡</sup> Department of Physics.

<sup>§</sup> Department of Biomedical Engineering.

<sup>||</sup> Department of Physical Chemistry.

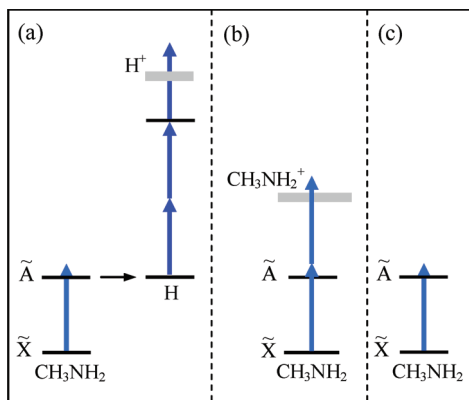


**Figure 1.** Schematic representation of the excitation processes for obtaining the (a) electronic H action spectrum in dissociation, (b) the resonantly enhanced two photon ionization spectrum, and (c) the absorption spectrum of methylamine.

shown in Figure 1. In the present measurements, methylamine was diluted to a  $\sim 3\%$  mixture with Ar at a total pressure of  $\sim 800$  Torr, expanded through a 0.8 mm orifice of a pulsed nozzle and skimmed  $\sim 2$  cm downstream the nozzle. The molecular beam traveled another  $\sim 3$  cm to the TOFMS interaction region, where it was intersected by the two laser beams. The typical working pressure was  $\sim 2 \times 10^{-6}$  Torr and the background pressure about 2 orders of magnitude lower.

The first UV beam (bandwidth =  $0.2 \text{ cm}^{-1}$ , energy  $\sim 150 \mu\text{J}$ ) in the 220–240 nm range was generated by the doubled output of a tunable dye laser, operated with different Coumarine dyes, which was pumped by the third harmonic of a Nd:yttrium–aluminum–garnet (YAG) laser. This beam was focused in the interaction region by a 30 cm focal length lens. Following the excitation pulse, after a delay of  $\sim 10$  ns, the probe beam was introduced into the region. This beam originates from a dye laser pumped by the second harmonic of another Nd:YAG laser. The output of this dye laser was frequency doubled and mixed with the fundamental of the Nd:YAG laser to produce light in the 243 nm wavelength region (bandwidth  $\sim 0.17 \text{ cm}^{-1}$ , energy  $\sim 200 \mu\text{J}$ ). The energy was kept at this low value to minimize other possible multiphoton processes. This beam was focused into the interaction region with a 30 cm focal length lens and employed for detection of the ensuing H photofragments by  $(2 + 1)$  resonantly enhanced multiphoton ionization (REMPI) via the two-photon transition,  $2s^2S \leftarrow 1s^2S$ , at 243.135 nm.

The H electronic action spectrum was obtained via the excitation scheme shown in Figure 1a, by monitoring the yield of the H atoms from the dissociation of methylamine while varying the wavelength of the electronic excitation laser and fixing the UV probe laser on the H two-photon transition. In addition, the same setup was used to obtain the resonantly enhanced two photon ionization (R2PI) spectrum of methylamine via the excitation scheme shown in Figure 1b, while using only the electronic excitation laser and scanning its wavelength.

Ions formed in the TOFMS interaction region via  $(2 + 1)$  REMPI or R2PI were subjected to continuously biased extraction, one acceleration stage, two pairs of orthogonal deflection plates and an Einzel lens prior to entering the field-free drift region and eventual detection by a microchannel plate. The ion signals were captured by a boxcar integrator and then directed via an analog to digital converter, to a personal computer controlling the data acquisition.

In addition, the  $\tilde{A} \leftarrow \tilde{X}$  absorption of methylamine in the same range was sampled by one-photon excitation, Figure 1c, through room temperature photoacoustic (PA) spectroscopy.<sup>20</sup> In this experiment, the UV beam ( $<90 \mu\text{J}$ ) was focused with a 10 cm focal length lens near a microphone in a PA cell with  $\sim 90$  Torr of methylamine.

**b. Computations.** The PESs for the N–H dissociation channel were calculated using the MOLPRO package,<sup>21</sup> employing the multireference configuration interaction method and the 6-31+G\* basis set. The active space, including two valence electrons distributed among five orbitals (three of them belonging to the  $A'$  irreducible representation) was used. Three electronic states were computed with equal weights. The one-dimensional PESs (based on the N–H stretch degree of freedom) were then modified using the vibrationally adiabatic approximation (VAA)<sup>22–25</sup> by adding the vibrational ground state energy of the second N–H bond (perpendicular oscillators). This approximation was employed since it was shown that it dramatically improves tunneling calculations of reduced dimensionality.<sup>26</sup> VAA corrections due to other degrees of freedom are expected to be small. For instance, our calculated VAA correction due to  $\text{CH}_3$  torsion changed the barrier height by only  $\sim 1.5\%$  and therefore was neglected.

Furthermore, these PESs were used to perform direct quantum dynamics calculations. These calculations were conducted while building artificial vibrational states on the  $\tilde{A}$  PES + VAA, representing different energy levels in the potential well. The wave functions of these states were allowed to propagate on the  $\tilde{A}$  PES + VAA for  $\sim 80$  fs. The wavepacket propagation was carried out by expanding the evolution operator to the Chebyshev series and applying this operator on the wave functions.<sup>27</sup> In addition, a complex absorbing potential<sup>28–32</sup> (CAP) was added to the PES + VAA at  $\text{N–H} = 3\text{--}6 \text{ \AA}$ , to avoid boundary reflections.

### III. Results and Discussion

**a. Different Spectra.** Figure 2 shows the measured H electronic action spectrum due to methylamine dissociation and the R2PI spectrum of methylamine [magenta and cyan traces in panels a and b, respectively]. It is clearly seen that as the wavelength of the electronic excitation laser varies, a sequence of peaks appears in the spectra, where their positions in the H electronic action spectrum mimic those in the R2PI spectrum. The R2PI spectrum, Figure 2b, resembles very much the corresponding spectrum measured by Kim and co-workers.<sup>16–18</sup> In fact, the observed peaks are related to the excitation of vibrationless ground state methylamine molecules on the  $\tilde{X}$  potential to resonant states on the  $\tilde{A}$  potential, corresponding to vibrational bands of  $\nu_7$  ( $\text{CH}_3$  rock),  $\nu_9$  ( $\text{NH}_2$  wag), and their combinations.<sup>16–18</sup> These resonances in the R2PI and H electronic action spectra arise from the predissociation of vibrational states of the bound potential surface via nonadiabatic coupling to the ground electronic PES.

It is worth noting that the signal intensity of the  $0_0^0$  band is about 2 orders of magnitude higher in the H action spectrum than in the R2PI spectrum under the conditions of our experiment. This implies that when methylamine is excited to the  $\tilde{A}$  state, the dissociation process where H atoms are released competes with the parent ionization, the former being much more efficient. This seems to hold for the conditions of our experiments, despite the fact that the molecular ion is dominant in the mass spectrum and its fragmentation is minimal.

In addition, although the positions of the peaks in the spectra are similar, it is clear that the intensity pattern observed in the

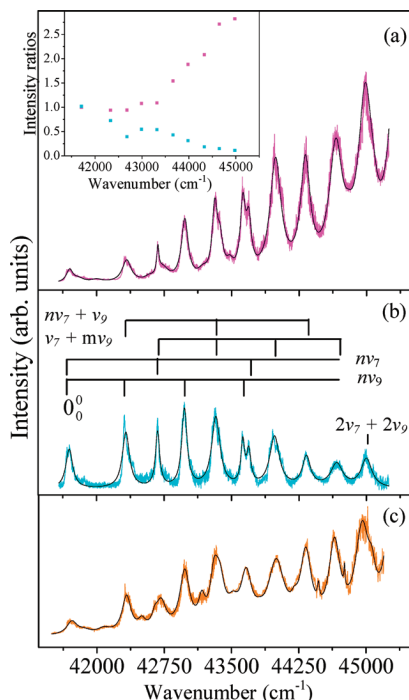


**Figure 2.** Traces represent the jet cooled (a) H photofragment electronic action spectrum of the dissociation (magenta), (b) the resonantly enhanced two photon ionization spectrum (cyan), and (c) the room temperature absorption spectrum (orange) of methylamine. The black spectra are the corresponding fitted ones, obtained from multiple Lorentzians. (b) also contains the assignment of the observed bands, based on ref 18. The inset in (a) includes the ratios of the yield of the H atoms and methylamine ionization to the intensities of absorption for individual bands (magenta and cyan, respectively) vs energy.

two types of spectra is very different. It is immediately apparent that the peak intensities in the R2PI spectrum decrease somewhat, while in the H electronic action spectrum they gradually increase for higher excitation energy. For example, the excitation of the  $2\nu_7 + 2\nu_9$  state, which is about  $3300\text{ cm}^{-1}$  higher than the  $0_0^0$  state, leads to about 30 times higher yield of H photofragments. This behavior could be related to different processes occurring as a result of methylamine excitation and their manifestation in the monitored spectra.

The electronic action and R2PI spectra were monitored with nanosecond pulses, which are significantly longer than the  $\tilde{A}$  state lifetime; nevertheless, it is assumed that these spectra are not significantly affected by the lifetime of individual bands. This is based on the fact that the lifetime at the origin of methylamine is  $\sim 0.38\text{ ps}$ , varying only a little upon vibrational energy increase; even the narrowest peak in the R2PI spectrum,  $\nu_7$ , exhibits a comparable lifetime of  $0.44\text{ ps}$ .<sup>17,18</sup> Furthermore, the first phases of the ionization and photodissociation processes of methylamine (see Figure 1), are similar, meaning that both spectra depend on the transition probability from the  $\tilde{X}$  ground electronic state to the  $\tilde{A}$  state and the Franck–Condon (FC) factors, which are set by the  $\text{NH}_2$  bent-to-planar structural change upon  $\tilde{A} \leftarrow \tilde{X}$  transition and the overlap integrals between the vibrational wave functions on the two involved electronic states, respectively. Therefore, it is reasonable to associate the difference between the two spectra with the dynamics following the excitation to the  $\tilde{A}$  state. Since earlier experiments and theoretical studies indicated that the dissociation of the hydrogen atom occurs by tunneling through an energy barrier,<sup>12,13,15–19</sup> it is reasonable to assume that the H yield is somewhat affected

by this tunneling. To test this possibility, the transmission coefficients, namely, the probability of the H atom to tunnel through the barrier should be calculated. It is anticipated that these coefficients could be obtained from the measured H electronic action spectrum, while accounting for the transition moments to individual bands.

Therefore, the absorption spectrum of methylamine, reflecting the cross section for excitation to the different vibronic states, was monitored [orange trace in Figure 2c]. This spectrum resembles the one measured using synchrotron radiation<sup>33</sup> and exhibits a vibrational structure that is characterized by rising intensity of the peaks. Although both the H electronic action [Figure 2a] and absorption spectra [Figure 2c] exhibit this type of behavior, their comparison shows that the H yield increase in the former is steeper, as higher resonant states on the  $\tilde{A}$  state are accessed, alluding to the effect of tunneling during N–H bond cleavage.

To quantify this effect, the H yield spectrum, representing the partial photodissociation cross section for H photofragment production, the R2PI spectrum, reflecting the ionization efficacy of the parent and the absorption spectrum, were fitted by multiple Lorentzian functions of variable widths, resulting in the black traces of Figure 2a–c, respectively. It is seen that these traces fit well the colored measured spectra and therefore the area of the Lorentzians in the different types of spectra correspond to the transition intensities and to the various processes occurring following excitation. It is thus expected that by calculating the ratio of the areas of the peaks exhibiting the H yield and the R2PI efficacy to those of the respective absorption peaks, the effect of the dynamics following the excitation to the  $\tilde{A}$  state could be unraveled. The obtained ratios thus allow roughly estimating the dependence of the N–H dissociation and methylamine ionization on the energy of the accessed vibronic states. These results are shown in the inset of Figure 2a, revealing H yield increase (magenta solid squares) and methylamine ionization decrease (cyan solid squares) as higher vibronic states on the  $\tilde{A}$  state are accessed. On the basis of previous studies,<sup>12,15–18</sup> it is thus assumed that the marked H yield increase and ionization decrease is a result of tunneling and that the solid squares are related to transmission coefficient, namely, the probability of the H atom to tunnel through the barrier. To verify this possibility, the experimental results are compared to calculated transmission coefficients, obtained by a simplified analytical model and by direct dynamics calculations.

**b. N–H Photodissociation through Tunneling.** Since the experimental data (see Figure 3) are assumed to indicate a smooth increase in H tunneling probability vs excitation energy, we analyze it by an analytical model, assuming a potential barrier of the form

$$U(x) = \frac{U_0}{\cosh^2(ax)} \quad (1)$$

where  $U_0$  is the potential barrier height,  $a$  its width parameter, and  $x$  is the reaction coordinate. The solution<sup>34</sup> of the corresponding Schrödinger equation gives the following functional form for the transmission coefficient,  $T$ :

$$T = \frac{\sinh^2(\pi k/a)}{\sinh^2(\pi k/a) + \cosh^2\left[\frac{1}{2}\pi\sqrt{8mU_0/\hbar^2 a^2 - 1}\right]} \quad (2)$$



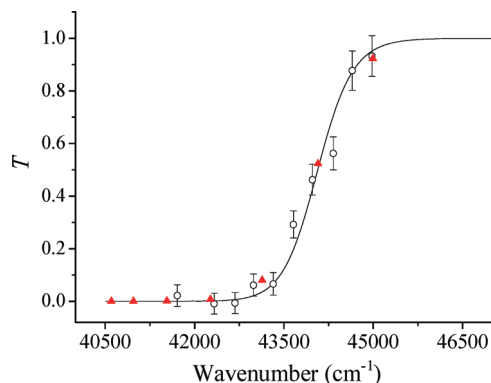


**Figure 3.** Transmission coefficient for tunneling of H atoms in cleavage of the N–H bond of methylamine, as a function of excitation energy: experimental (open circles), direct dynamics calculations (triangles), and fit with the transmission function of a hyperbolic cosine potential (line).

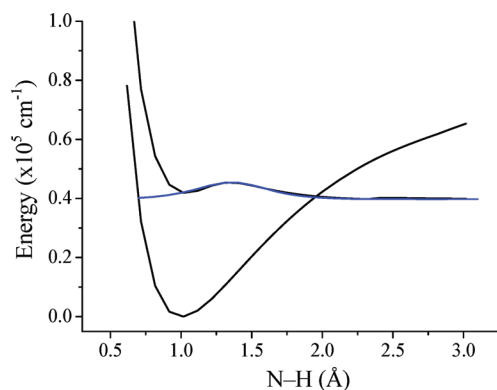


**Figure 4.**  $\tilde{X}$  and  $\tilde{A}$  potential energy surfaces (PESs) ( $\tilde{A}$  includes the vibrational adiabatic approximation (VAA)) for the N–H dissociation channel of methylamine, where both states belong to  $C_s$  symmetry. Also shown is the fitted hyperbolic cosine potential (blue trace) of eq 1 to the  $\tilde{A}$  PES + VAA, with the  $U_0$  and  $a$  parameters of 5726  $\text{cm}^{-1}$  and 3.0  $1/\text{\AA}$ , respectively.

where  $k = (2mE)^{1/2}/\hbar$  and  $E$  is the energy of the tunneling particle. Although this hyperbolic cosine barrier is one of many possible choices of smooth barriers, we preferred to select it since its analytical solution is known, giving us the opportunity to obtain a convincing, yet simple interpretation of the experimental results.

The transmission coefficient is expected to describe in our case the probability of N–H bond breaking in methylamine, provided that the dissociation probability of the H atoms that tunnel through the barrier is high. This seems very reasonable considering that the H atoms that already tunneled approach the point of CI<sup>15</sup> or the line of CIs<sup>16</sup> and undergo fast dissociation. The dependence of  $T$  on the excitation energy is exhibited by an “S”-shaped curve, shown in Figure 3. This S-shaped curve, eq 2, was obtained by fitting the hyperbolic cosine potential, eq 1, using values of 5726  $\text{cm}^{-1}$  and 3.0  $1/\text{\AA}$  for  $U_0$  and  $a$ , respectively, to the calculated N–H bond fission path on the PES + VAA of the  $\tilde{A}$  state ( $C_s$  symmetry), Figure 4. By comparing this S-curve with the experimental data, while obtaining the best fitting for the bottom of the well and for a single normalization constant (takes care to show all data points on a scale corresponding to the S-shaped curve), we obtained the matching shown in Figure 3. It is clear that the calculated S-shape curve reproduces well the measured H yield, showing that the increase in yield could be a result of tunneling, sustaining previous findings and suggestions.<sup>12,15–18</sup>

Further support to the fact that the photodissociation process involves tunneling was gained from the results of direct one-dimensional dynamics calculations. The red triangles in Figure 3 exhibit these results, showing the percentage of the wave function absorbed by the CAP (after  $\sim 80$  fs) as a function of the initial energy level. It is apparent that these results fit well both the experimental results and the analytical S-curve.

The results obtained through the use of a simplified model of the potential barrier, fitting the calculated PES + VAA and the direct dynamics calculations on the PES + VAA, and their agreement with the experimental data imply that the enhanced dissociation is a result of tunneling through a barrier. This seems very reasonable, provided that the bound region of the  $\tilde{A}$  state PES and therefore the accessed resonances are energetically situated above the CI (see Figure 4). Consequently, it is anticipated that H atoms that tunnel through the barrier will easily approach the point of CI,<sup>15</sup> or even more so the line of CIs<sup>16</sup> leading to the N–H bond rupture.

#### IV. Conclusions

We have studied the quantum tunneling of H atoms formed during methylamine predissociation. The system under investigation consists of a bound electronic state having quantum mechanical resonances and coupling with the ground electronic state through CI.<sup>15,16</sup> An increase in H atom release and decrease in the competing channel of methylamine ionization was observed while higher resonances on the first electronic bound state were accessed. The comparison between the experiment and the results of the analytical model and the direct dynamics calculations is rather convincing evidence that the release of H atoms in N–H bond fission of methylamine is due to resonance enhanced quantum tunneling.

**Acknowledgment.** Financial support from the Israel Science Foundation founded by The Israel Academy of Science and Humanities and the James Franck Binational German-Israeli Program in Laser-Matter Interaction is gratefully acknowledged.

#### References and Notes

- (1) Ashfold, M. N. R.; Bagott, J. E. *Molecular Photodissociation Dynamics, Advances in Gas-Phase Photochemistry and Kinetics*; Royal Society of Chemistry: London, 1987.
- (2) Schinke, R. *Photodissociation Dynamics*; Cambridge University Press: Cambridge, U.K., 1993.
- (3) Butler, L. J.; Neumark, D. M. *J. Phys. Chem.* **1996**, *110*, 12801.
- (4) Crim, F. F. *J. Phys. Chem.* **1996**, *100*, 12725.
- (5) Bar, I.; Rosenwaks, S. *Int. Rev. Phys. Chem.* **2001**, *20*, 711.
- (6) Sato, H. *Chem. Rev.* **2001**, *101*, 2687.
- (7) Kawasaki, M.; Bersohn, R. *Bull. Chem. Soc. Jpn.* **2002**, *75*, 1885.
- (8) Levine, R. D. *Molecular Reaction Dynamics*; Cambridge University Press: Cambridge, U.K., 2005.
- (9) Rosenwaks, S. *Vibrationally Mediated Photodissociation*; Royal Society of Chemistry: Cambridge, U.K., 2009.
- (10) Michael, J. V.; Noyes, W. A. *J. Am. Chem. Soc.* **1963**, *85*, 1228.
- (11) Waschewsky, G. C. G.; Kitchen, D. C.; Browning, P. W.; Butler, L. J. *J. Phys. Chem.* **1995**, *99*, 2635.
- (12) Ashfold, M. N. R.; Dixon, R. N.; Kono, M.; Mordaunt, D. H.; Reed, C. L. *Philos. Trans. R. Soc. London A* **1997**, *355*, 1659. Reed, C. L.; Kono, M.; Ashfold, M. N. R. *J. Chem. Soc., Faraday Trans.* **1996**, *92*, 4897.
- (13) Marom, R.; Zecharia, U.; Rosenwaks, S.; Bar, I. *Mol. Phys.* **2008**, *106*, 213; *J. Chem. Phys.* **2008**, *128*, 154319. Marom, R.; Weiss, T.; Rosenwaks, S.; Bar, I. *J. Chem. Phys.* **2009**, *130*, 164312.
- (14) Marom, R.; Weiss, T.; Rosenwaks, S.; Bar, I. Unpublished work.
- (15) Dunn, K. M.; Morokuma, K. *J. Phys. Chem.* **1996**, *100*, 123.
- (16) Levi, C.; Halász, G. J.; Vibók, Á.; Bar, I.; Zeiri, Y.; Kosloff, R.; Baer, M. *J. Chem. Phys.* **2008**, *128*, 244302; *Int. J. Quantum Chem.* **2009**, *109*, 2482; *J. Phys. Chem. A* **2009**, *113*, 6756. Levi, C.; Kosloff, R.; Zeiri, Y.; Bar, I. *J. Chem. Phys.* **2009**, *131*, 064302.
- (17) Baek, S. J.; Choi, K.-W.; Choi, Y. S.; Kim, S. K. *J. Chem. Phys.* **2002**, *117*, 10057.

- (18) Baek, S. J.; Choi, K.-W.; Choi, Y. S.; Kim, S. K. *J. Chem. Phys.* **2003**, *118*, 11026.
- (19) Park, M. H.; Choi, K.-W.; Choi, S.; Kim, S. K. *J. Chem. Phys.* **2006**, *125*, 084311.
- (20) West, G. A.; Barrett, J. J.; Siebert, D. R.; Reddy, K. V. *Rev. Sci. Instrum.* **1983**, *54*, 797.
- (21) Werner, H.-J.; Knowles, P. J.; Amos, R. D.; Bernhardsson, A.; Berning, A.; Celani, P.; Cooper, D. L.; Deegan, M. J. O.; Dobbyn, A. J.; Eckert, F.; Hampel, C.; Hetzer, G.; Knowles, P. J.; Korona, T.; Lindh, R.; Lloyd, A. W.; McNicholas, S. J.; Manby, F. R.; Meyer, W.; Mura, M. E.; Nicklass, A.; Palmieri, P.; Pitzer, R.; Rauhut, G.; Schutz, M.; Schumann, U.; Stoll, H.; Stone, A. J.; Tarroni, R.; Thorsteinsson, T.; Werner, H.-J. MOLPRO, version 2002.6.
- (22) Marcus, R. A. *J. Chem. Phys.* **1966**, *45*, 4493.
- (23) Wyatt, R. E. *J. Chem. Phys.* **1969**, *51*, 3489.
- (24) Truhlar, D. G. *J. Chem. Phys.* **1970**, *53*, 2041.
- (25) Miller, W. H. In *Tunneling*; Jortner, J., Pullman, B., Eds.; D. Reidel: Dordrecht, The Netherlands, 1986; p 91.
- (26) Baer, R.; Zeiri, Y.; Kosloff, R. *Phys. Rev. B* **1996**, *54*, R5287.
- (27) Kosloff, R. In *Dynamics of Molecules and Chemical Reactions, in Dynamics of Molecules and Chemical Reactions*; Wyatt, R. E., Zhang, J. Z., Eds.; Marcel Dekker: New York, 1996; p 185.
- (28) Leforestier, C.; Wyatt, R. E. *J. Chem. Phys.* **1983**, *78*, 2334.
- (29) Kosloff, R.; Kosloff, D. *J. Comput. Phys.* **1986**, *63*, 363.
- (30) Riss, U. V.; Meyer, H.-D. *J. Phys. B* **1993**, *26*, 4503.
- (31) Riss, U. V.; Meyer, H.-D. *J. Chem. Phys.* **1996**, *105*, 1409.
- (32) Vibok, A.; Balint-Kurti, G. G. *J. Chem. Phys.* **1992**, *96*, 7615.
- (33) Hubin-Franskin, M.-J.; Delwiche, J.; Giuliani, A.; Ska, M.-P.; Motte-Tollet, F.; Walker, I. C.; Mason, N. J.; Gingell, J. M.; Jones, N. C. *J. Chem. Phys.* **2002**, *116*, 9261.
- (34) Landau, L. D.; Lifshitz, E. M. *Quantum Mechanics*, 3rd ed.; Pergamon Press: Oxford, U.K., 1977.

JP912107H